Colloids and Surfaces A: Physicochem. Eng. Aspects 416 (2013) 9–15

Contents lists available at SciVerse ScienceDirect

Colloids and Surfaces A: Physicochemical and Engineering Aspects

journal homepage: www.elsevier.com/locate/colsurfa

Modification of polycrystalline nanodiamonds by using periodic magnetic field enhanced hydrogen plasma and the application on nanogrinding of thin film magnetic head

Xuezhang Liu[a], Zhiming Yu[a,b,*], Qiuping Wei[a,b,*], Guofeng Wen[c], Xiaohua Duan[d], Xiaolong You[a]

[a] School of Materials Science and Engineering, Central South University, Changsha, 410083, PR China
[b] State Key Laboratory of Powder Metallurgy, Central South University, Changsha, 410083, PR China
[c] SAE Technologies Development Co., Ltd, Dongguan, 523087, PR China
[d] Changsha Telecommunications and Technology Vocational College, Department of Computer and Information Engineering, Changsha, 410015, PR China

HIGHLIGHTS

- ► Modification of polycrystalline nanodiamonds by using PMF enhanced H_2 plasma.
- ► The enhancement mechanism of PMF on H_2 plasma modification was clarified.
- ► Well-dispersed nanodiamonds in clean oil have been prepared.
- ► The application on nanogrinding of thin film magnetic head was testified.
- ► A smooth substrate ($R_a \sim 0.387$ nm, $PTR \sim 0.048$ nm) was achieved.

GRAPHICAL ABSTRACT

By modifying diamond nanoparticles with PMF enhanced H2 plasma in the gas phase, well-dispersed and stable suspensions of polycrystalline NDs in clean oil medium can be prepared. As can be seen from the SEM image, most of the particles are basically spherical or near spherical and the size distribution is approximately 80–100 nm. The adhesion covered diamond nanoparticles is residual clean oil, which cannot be volatilized.

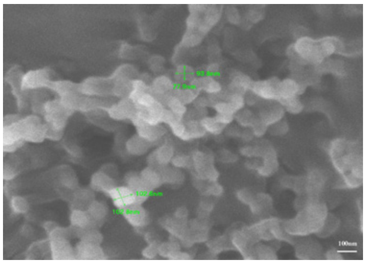

ARTICLE INFO

Article history:
Received 30 July 2012
Received in revised form
24 September 2012
Accepted 11 October 2012
Available online xxx

Keywords:
Nanodiamond
Periodic magnetic field
Hydrogen plasma
Dispersion
Thin-film magnetic head
Nanogrinding

ABSTRACT

Polycrystalline nanodiamonds (NDs) derived from shock wave synthesis exhibits serious agglomeration in non-polar medium such as clean oil. Here we report an efficient new approach to modify the NDs by exposing the nanoparticles to periodic magnetic field (PMF) enhanced hydrogen plasma in the gas phase. The modification treatment transforms oxygenated groups on the NDs surface into C—H terminations. The evolution of polycrystalline NDs has been carefully characterized by FTIR, Raman and XRD analysis and the enhancement mechanism of PMF was discussed. After this treatment, well-dispersed and stable suspensions of diamond nanoparticles in clean oil with average diameter of 74.7 nm can be obtained. Subsequent nanogrinding of thin-film magnetic heads (TFH) validates their dispersion behavior. A smooth substrate ($R_a \sim 0.387$ nm) surface and a planar recording surface ($PTR \sim 0.048$ nm) were achieved.

---

* Corresponding authors at: School of Materials Science and Engineering, Central South University, Changsha, 410083, PR China. Tel.: +86 731 88830335; fax: +86 731 88876692.
E-mail addresses: zhiming@csu.edu.cn (Z. Yu), qiupwei@csu.edu.cn (Q. Wei).

0927-7757/$ – see front matter
http://dx.doi.org/10.1016/j.colsurfa.2012.10.024

1. Introduction

Diamond nanoparticles or nanodiamonds (NDs) have attracted considerable interest among researchers recently due to their potential applications in the fields of catalysis [1], biological systems [2] and electronic applications [3]. However, as reported in the literature [4], the physical properties of nanodiamond surface are strongly affected and determined by adsorbed species and their bonding configuration, surface impurities and morphology. The extent of H and O surface termination has a profound effect on the wettability [5], charge density [6], and surface electronic properties [7]. Photoemission of boron-doped H-terminated diamond single crystals are characterized by a negative electron affinity (NEA) in the range of −1.3 to −1.0 eV, while oxygenation of the surfaces by a hot acid treatment leads to a positive electron affinity (PEA) between 1.4 and 1.7 eV [2,8]. An essential prerequisite for these applications is the control of surface structure and agglomeration.

By exposition to atomic hydrogen under ultra-high vacuum (UHV) [9], microwave hydrogen plasma [10] or microwave plasma chemical vapor deposition (MPCVD) [11], oxygenated terminations on NDs surface can be homogenize into C—H groups. Girard et al. [11] even obtained the whole hydrogenation of the NDs surface by MPCVD. While, in a conventional MPCVD system, atomic hydrogen in plasma can etch the quartz wall and grown films are consequently contaminated with etched silicon. To suppress this contamination, researchers have begun to use stainless steel reaction chambers whose inner diameter is sufficiently large to avoid the plasma coming into contacting with it. But exchanging the stainless chamber is not an easy and inexpensive task [12].

Here, we report a new approach to the modification of nanodiamonds by periodic magnetic field (PMF) enhanced hydrogen plasma. The rotating magnetic field can improve the spatial distribution of hydrogen plasma and keep charged particles in the plasma away from the vacuum chamber wall [13].

Polycrystalline nanodiamonds derived from shock wave synthesis have been studied in this paper [14,15]. They possess characteristics of sphere shape, chemical stability and self-sharpening [16]. Compared with monocrystalline diamond particles produced by high pressure high temperature (HPHT), polycrystalline NDs can resist fracturing along certain crystallographic cleavage planes [16,17]. All of those virtues ensure them an ideal abrasive for TFH nanogrinding [18]. Unfortunately, like other nanoscale powders, polycrystalline NDs tend to form larger agglomeration to minimize its surface energy, which retards their dispersion behavior in nonpolar medium such as clean oil. The agglomeration ranging from hundreds of nanometers to micrometer is likely facilitated by the formation of the ethereal group ($\geqslant$C—O—C$\leqslant$) between particles due to the presence of oxygen-containing groups on the NDs surface. Atomic hydrogen treatment can passivate the surface by saturating the dangling bonds of the surface carbon atoms with hydrogen-containing groups and thus prevent particles from the subsequent aggregation [9].

The evolution of polycrystalline NDs induced by PMF enhanced hydrogen plasma was carefully characterized by FTIR, Raman and SEM. The dispersion behavior of treated powders in clean oil and subsequent TFH nanogrinding were investigated.

2. Experiment

2.1. Chemicals

Polycrystalline NDs with phase purity higher than 95% was purchased from Beijing Li-Xin Mechanical and Electric High Technology Company (China). Nominal mean particle size of the powders is 100 nm in diameter. The surface area measured by nitrogen gas adsorption is 284.5 $m^2 g^{-1}$. Clean oil with kinematic viscosity around 5 $mm^2 s^{-1}$ (40 °C) was adopted as suspension medium. Flash point (open) of the medium is high than 110 °C, while pouring point is lower than −5 °C.

2.2. Modification treatment

In a typical modification process, 200 mg of polycrystalline NDs was loaded in the reactor of PMF enhanced chemical vapor deposition system. The system consists of a quartz chamber, a three-phase stator winding and an AC transducer. The PMF, with $B = B_0 \sin \omega t$, is generated by the stator winding of a three-phase electric motor. Details of the experimental set-up can be found elsewhere [13]. After a pumping stage, the hydrogen was injected up to 3 Kp_a and hydrogen plasma was thermally activated by a tungsten filament above the polycrystalline NDs. While angular frequency (ω) of PMF was adjusted at 3000 rpm, the corresponding magnetic field was 106 Gauss. Polycrystalline NDs was treated for 30 min after the temperature reached 873 ± 50 K. The temperature was measured by a thermocouple set on the surface of sample. Before the powder was taken out of the reaction chamber for further investigation, the sample was cooled under hydrogen atmosphere.

2.3. Nanogrinding

Modified polycrystalline NDs were dispersed in clean oil for nanogrinding by using a direct-immersion horn-type ultrasound sonicator (output power: 400 W, time: 30 min). A tin plate was machined by super precision numeric lathe, cut spiral groove on the plate surface, and then grounded by condition ring with clean oil. After being removed burr, the lap plate was charged with the polycrystalline NDs suspension. The charging process involves a ring riding on the surface of the plate, while the suspension was spayed to the plate an appropriate interval. The diamond nanoparticles in the slurry were sandwiched between the ring and the plate and charged to the plate [19]. A float-piece polisher with condition ring was used in this investigation.

2.4. Characterizations

Fourier transform infrared (FTIR) spectroscopy was introduced to analyze the functional groups of polycrystalline NDs surface. The spectra were recorded in air with *Nexus* 470 (Thermo Nicolet, USA) in the range of 4000–450 cm^{-1}. Resolution of the spectroscopy was equal to 4 cm^{-1}. The number of scans was 16 and scan step was 11.9 cm^{-1}. X-ray diffraction (XRD) analysis was conducted by using diffractometer D/*max-r*A (Rigaku, Japan) with Cu radiation. Raman spectra were also recorded in air by a micro-Raman spectroscopy (Lab Raman RH800) using an Ar^+ ion laser (488 nm) at 800–2000 cm^{-1}. Prior to Raman characterization of the powders, the Raman system was calibrated by a Si wafer.

The morphology of polycrystalline NDs was characterized by field emission scanning electron microscope (FE-SEM, FEI Sirion200) with energy dispersive X-ray detector (EDX), while particle size analyzer (HORIBA, LB-550) was adopted for the measurement of size distribution. Atomic force microscopy (AFM, Nanoscope IIIa from Veeco) operating in tapping mode with silicon cantilevers (nominal radius of 10 nm) was used to characterize the surface topography of finish surface.

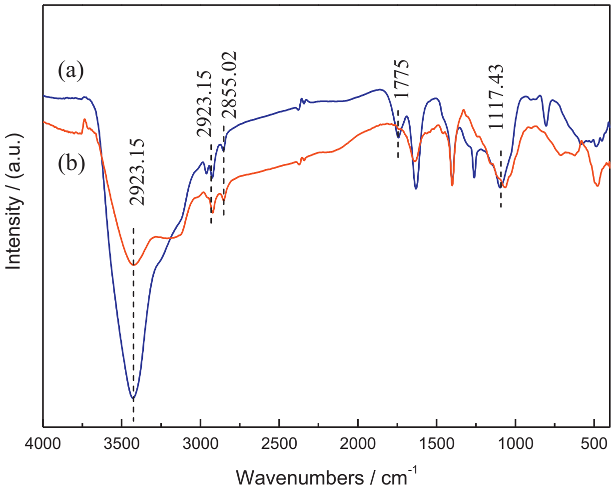

Fig. 1. FTIR spectra of as-received (a) and modified polycrystalline NDs with PMF enhanced H_2 plasma (b).

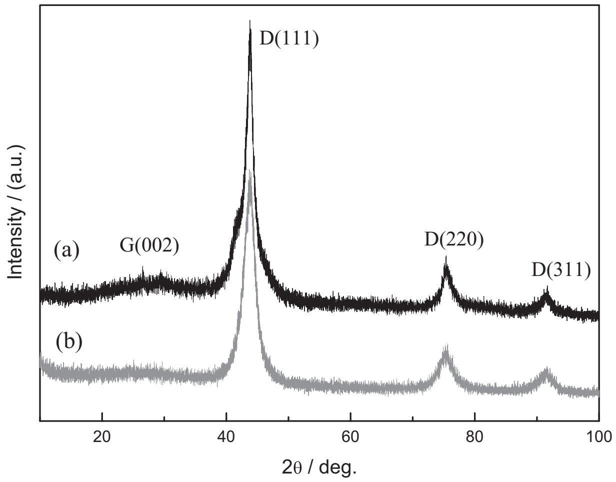

Fig. 2. XRD patterns of as-received (a) and modified polycrystalline NDs with PMF enhanced H_2 plasma (b).

3. Results and discussion

3.1. Modification treatment

The transformation of surface functional groups on polycrystalline NDs by PMF enhanced hydrogen plasma was investigated by FTIR spectroscopy in air. As illustrated in Fig. 1, the absorption peaks at 2923.16 and 2855.02 cm^{-1} corresponds to the asymmetric and symmetric stretching C—H vibration, respectively. And the absorption peak at 3433.76 cm^{-1} corresponds to the stretching O—H vibration, which is rather sensitive to the humidity of the samples [8,20]. The absorption peak at 1117.43 cm^{-1} corresponds to the deformation O—H vibration. The strong signal in the range of 1000–1250 cm^{-1} is linked to nitrogen impurities as well as C—O—C groups at the particle surface. A broad band observed at 1775 cm^{-1} is the characteristic of C═O stretching band involved in carboxylic acid groups and anhydride functionalities. After treated with PMF enhanced H_2 plasma, the peak of C═O stretching band between 1600 and 1800 cm^{-1} disappears, while the C—H stretching peaks between 2923.16 and 2855.02 cm^{-1} become sharper. The evolution of the particle surface termination in our experiments coincides with other works [8,11], where the NDs were hydrogenated by using MPCVD.

XRD analysis is performed to study the effect of modification treatment on the crystalline structure of nanoparticles. Diffraction patterns for as-received and modified samples are shown in Fig. 2. When the scan angle 2θ is ranging from 10° to 100°, characteristic intense diffraction peaks of diamond are observed in both samples at 44°, 76° and 92°, which agree well with the corresponding (1 1 1), (2 2 0) and (3 1 1) reflections. A broad peak at about 26° for as-received sample implies the presence of graphite residue after purification. After modified upon PMF enhanced H_2 plasma, this graphite peak is removed, while no modification of any diamond peak is observed. Average crystallites sizes calculated from FWHM using Scherrer formula give a diameter of 10.4 nm and 10.3 nm for polycrystalline NDs before and after the hydrogenation, respectively [16]. Those results thus confirm that this treatment is restricted to the sample surface.

Both of the particle samples were further examined by Raman spectra to determine the phase transformation. The results are shown in Fig. 3. The Raman peaks at approximately 1323 and 1560 cm^{-1} are assigned to diamond phase and G-band of graphite respectively. Both of the diamond and graphite peaks have a considerable width, which can attribute to the small size effects of the grains. After PMF enhanced H_2 plasma treatment, the diamond peak becomes sharper, which implies the improvement of diamond crystallinity. The intensity of the broad peak related to graphite slightly turns to be weaker. Despite the absence of graphite diffraction peak in the XRD pattern (Fig. 2), it can be clearly distinguished in Raman spectroscopy because the scattering intensity of graphite is about 60 times of diamond [21]. Our results reveal that PMF enhanced H_2 plasma treatment cannot totally remove the amorphous carbon impurities from the dynamically synthesized diamond. Pengwan Chen et al. [16] speculate that this part of amorphous carbon is transformed from the diamond and forms a mantle outside the diamond crystals, and some of their atoms are trapped by diamond lattice (Fig. 4).

3.2. The enhancement of PMF on H_2 plasma treatment

In conventional hot-filament chemical vapor deposition (HFCVD) system, the H_2 gas is thermally activated by an incandescent filament. H_2 molecules dissociate at the HF surface. Once away from the hot near filament region, the H atom concentration drops quickly as a result of H abstraction and recombination and then causes non-uniform [22].

Whereas applying a PMF upon chemical vapor deposition system, the direction and the strength of PMF change with time.

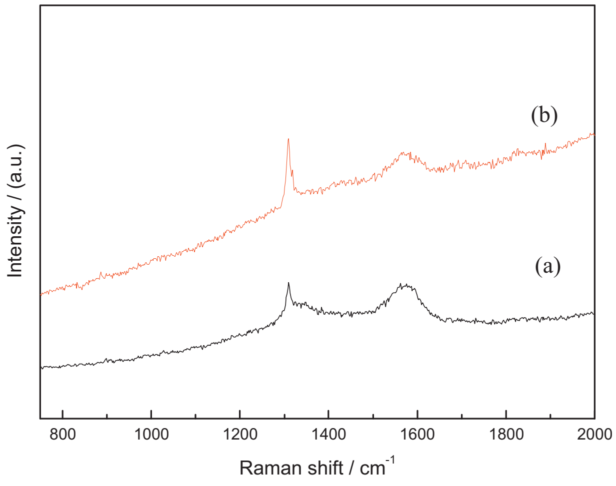

Fig. 3. Raman spectra of as-received (a) and modified polycrystalline NDs with PMF enhanced H_2 plasma (b).

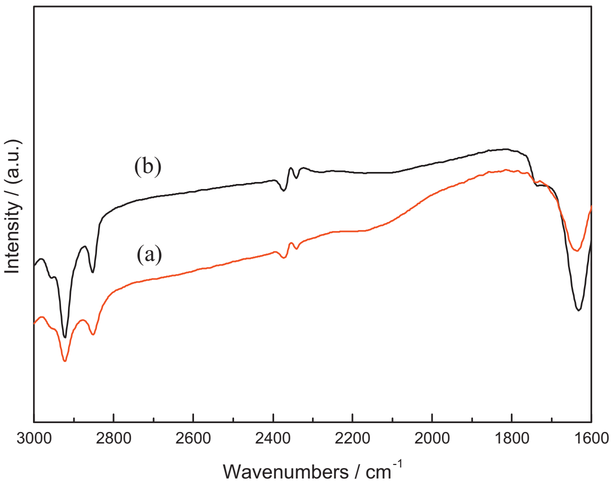

Fig. 4. FTIR spectra of modified polycrystalline NDs with PMF (a) and without PMF enhanced H_2 plasma (b).

It caused the electrons (emitted from the HF) to move in a spiral involution before they vanished or recombined, enhancing the probability of collision between electrons and H_2 molecules, and producing more ionization. It conspicuously improves the non-uniform of gas chemistry [13]. More importantly, the PMF engenders a self-excited electric field. The direction of electric field synchronously changes with the PMF. It accelerates charged particles (e, $H^\bullet$ and H^+) to bombard the powders, which decreases the energy barrier for the rupture reaction of oxygenated functional groups. While the reaction kinetics for oxygenated groups on the surface of polycrystalline NDs must be very complicated, we need more investigation to quantify the effect of PMF by theoretical calculation.

Fig. 5 presents FTIR spectra of polycrystalline NDs powders modified with PMF and without PMF enhanced H_2 plasma under the same temperature. When plotting the data, the wavenumbers range was shortened to improve the readability of the spectra. For polycrystalline NDs powders modified with PMF enhancement, the peak of C=O stretching vibration of carbonyl groups are less more intense after 30 min treatment at 873 ± 50 K. While, for polycrystalline NDs powders without PMF enhancement, the peak of C=O stretching vibration of carbonyl groups is still distinct. This result demonstrates the enhancement of PMF on the NDs modification. Korolkov et al. [23] reported that stream hydrogenation was performed at 1073 K for 5 h to reduce the oxygen-containing groups of DND surface. By comparison, we can perform hydrogenation modification at medium temperature.

3.3. Dispersion in clean oil

When as-received powders are dispersed in clean oil by using a direct-immersion horn-type ultrasound sonicator, serious aggregation and sedimentation are observed. Size distribution measured by dynamic light scattering method can be found in Fig. 5a. As the agglomeration exists, the size distribution of ND particles in clean oil is quite broad and only 45.2% of particles are smaller than 100 nm. After PMF enhanced H_2 plasma treatment, the aggregates disappeared entirely and the distribution comparatively became narrow. Particle size distribution illustrates that 97.6% of particles are smaller than 100 nm in dimension, while the average size is 74.4 nm.

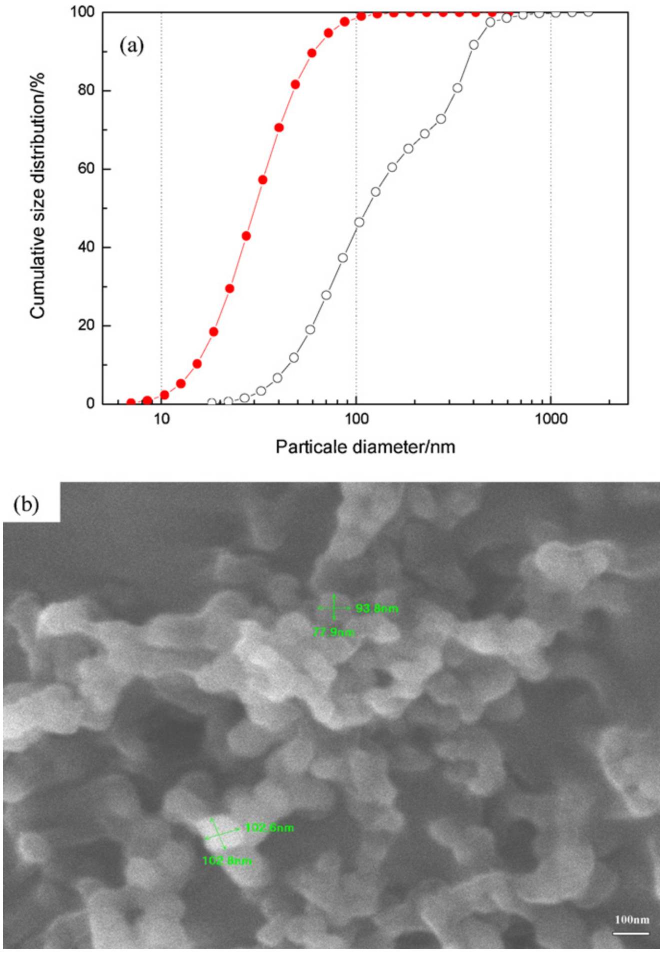

Fig. 5. (a) Particle size distribution of polycrystalline NDs, where hollow circle is corresponded to as received powders; solid circle is corresponded to modified sample. (b) SEM images of modified powders dispersed in clean oil.

A droplet of polycrystalline NDs suspension was spread out on a copper substrate. Since copper has excellent conductivity, we can observe individual particles directly. Fig. 5b provides more detailed data on the size and shape of diamond nanoparticles. As can be seen from the SEM images, most of the particles are basically spherical or near spherical and the size distribution is approximately 80–100 nm (in agree with PCS analysis data). A few larger particles, aggregations of the smaller ones, can be observed, but the whole particles are well-dispersed. The adhesion covered diamond nanoparticles is residual clean oil, which cannot be volatilized. Furthermore, Fig. 5b also confirms that the integrity of the particles is not compromised by H_2 plasma treatment.

In clean oil with low dielectric constant, the ionization of powders' functional groups is not so obvious. Then, the contribution of electrostatic repulsion between adjacent particles is limited and is no longer the main mechanism of particle dispersion [5]. On one hand, after modification treatment, hydrophilic groups presented initially on polycrystalline NDs surface, including carboxylic and hydroxyl groups, were replaced by C—H terminated ones. The changes of surface functional groups are proved by FTIR analysis. This treatment improves the wettability of diamond nanoparticles in clean oil. On the other hand, hydrogenation treatment passivates the surface and reduces the bonding between nanoparticles [9]. With high energy ultrasonic, those particles can be highly dispersed in clean oil. By the methods of milling process or chemical modification [24–26], nanodiamond can also be dispersed in nonpolar solvent, but those diamond nanoparticles are unavoidably contaminated by milling beads or surfactants.

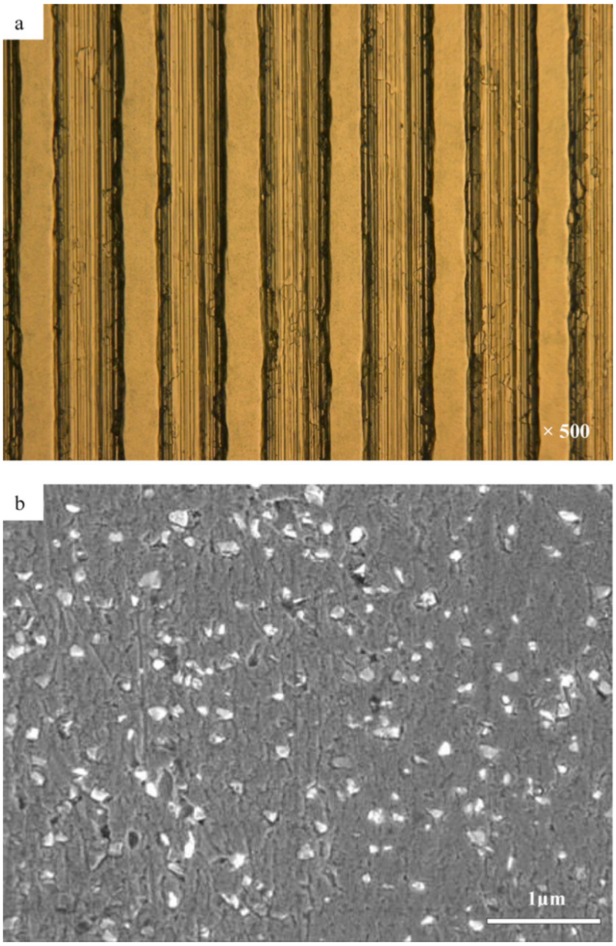

Fig. 6. Tin plate charged with modified polycrystalline NDs was examined by optical microscope (a) and scanning electron microscopy (b), respectively.

3.4. TFH nanogrinding

For a TFH, pole tip is only 20 μm away from one edge, so the edge roll-off is forbidden in abrasive finishing [27]. A soft metal plate, tin alloy plate was used in this experiment for its appropriate rigidity and good holding ability of abrasive particles. Fig. 6a shows the plate surface after charging process. Inspected by an optical microscope with a magnification of 500×, polycrystalline NDs were charged into ridges without damaging the surface quality of the tin plate surface. No scratches presents in the ridges. Fig. 6b is a SEM image of the plate surface. As the image revealing, diamond nanoparticles are uniformly dispersed in plate surface. While parts of the grains are embedded in the tin plate and other parts remains out of the tin surface. No serious aggregations appear. Those results demonstrate the perfect dispersion of modified nanoparticles in clean oil.

Fig. 7a shows the pole tip of TFH after grinding by as-received powders. It presents two types of surface defects: micro scratches and black spot. Those defects are common in the TFH surface grinded by micro-scaled diamond, which are detrimental to the production yield. EDX analysis was carried out to investigate the element composition of black spot. The result is shown in Fig. 7b. Four elements, Fe, Co, Ni and C were detected. The former three must be originated from pole tip material [27]. The presence of C signal implies that there is diamond nanoparticles embedded in pole tip.

A SEM of the TFH grinding by modified powders is depicted in Fig. 8. The SEM image shows that the finishing surface is smooth.

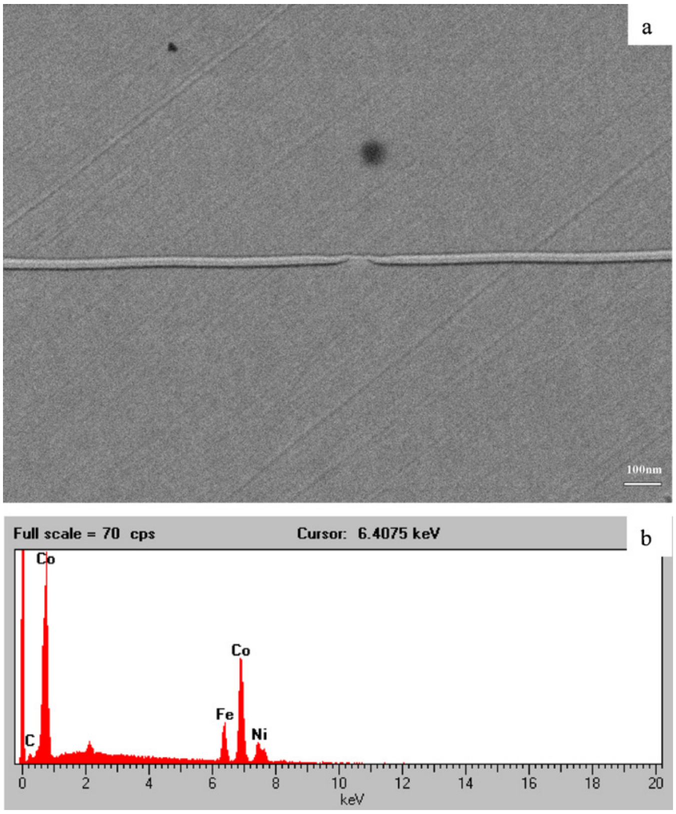

Fig. 7. The SEM image of pole tip area after nanogrinding by as received polycrystalline NDs (a) and EDX analysis on black spot (b).

No black spot can be tested. To obtain a complete understanding of surface topography, AFM were performed on two pole tips. The roughness (R_a) is 0.723 nm and 0.387 nm, respectively (Table 1). The topographies are presented in Fig. 9.

Since R_a alone is not adequate to assess the surface topography as different surface profiles can exhibit similar roughness values [28], the surface skewness (R_{sk}) is also listed in Table 1. The surface skewness is a statistical term describing the third central moment of the height values about the mean height and is a measure of the surface asymmetry [29]. Positive values of the surface skewness are found for flat surfaces with peaks, whereas negative values are

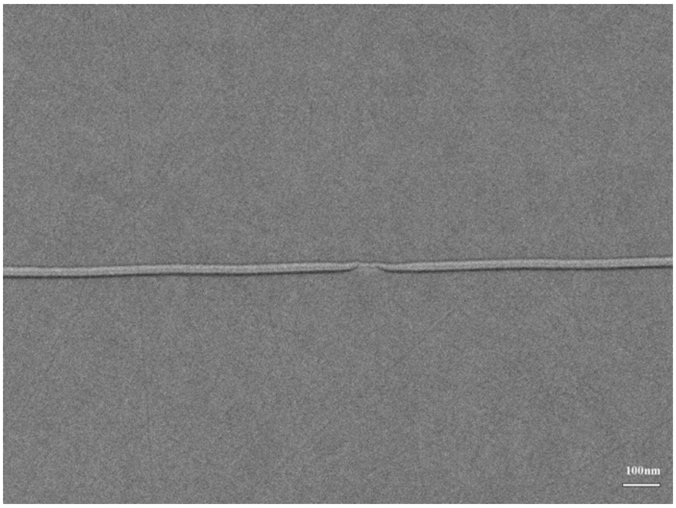

Fig. 8. The SEM image of pole tip area after nanogrinding by modified polycrystalline NDs.

Table 1
Statistics of surface topographies.

Specimen no.	R_{pv} (nm)	R_q (nm)	R_a (nm)	R_z (nm)	R_{sk}	R_{su}
D1[a]	7.794	0.969	0.723	7.069	1.194	4.977
D2[b]	3.835	0.483	0.387	3.425	−0.024	2.943

[a] TFH after nanogrinding by as-received powders.
[b] TFH after nanogrinding by modified powders.

representative of bearing surfaces with holes. Values numerically greater than 1.0 may indicate extreme holes or peaks on surfaces. R_{sk} are 1.194 nm and −0.024 nm for THFs after nanogrinding with as-received powders and modified one, respectively. It indicates that less asymmetric height distributions achieved by modified diamond nanoparticles are obtained.

In nanogrinding, abrasive particles are embedded in a lapping plate and a lubricant is passed between the workpiece and the lapping plate [18]. Obviously, the charging process is the critical process. The improvement of surface quality must chiefly be attributed to the dispersion of nanoparticles in clean oil. The suspension with good dispersion and short size distribution can ensure nanoparticles uniformly embedding in tin plate. However, when diamond with bad dispersion is employed, some big aggregations formed by lots of small particles will be charged into tin plate as one individual grain. It will bring two types of potential dangers. One is that aggregation cuts the TFH surface with bigger scratch. The other is that such aggregation lack of structural strength will be smashed into small particle and free roll on the plate under the collision of friction force. It can change nanogrinding into free abrasive grinding and finally decrease finishing surface. Moreover, free abrasive also tends to embed into pole tip since the material of pole tip is soft. Then, micro scratches and black spot are avoided.

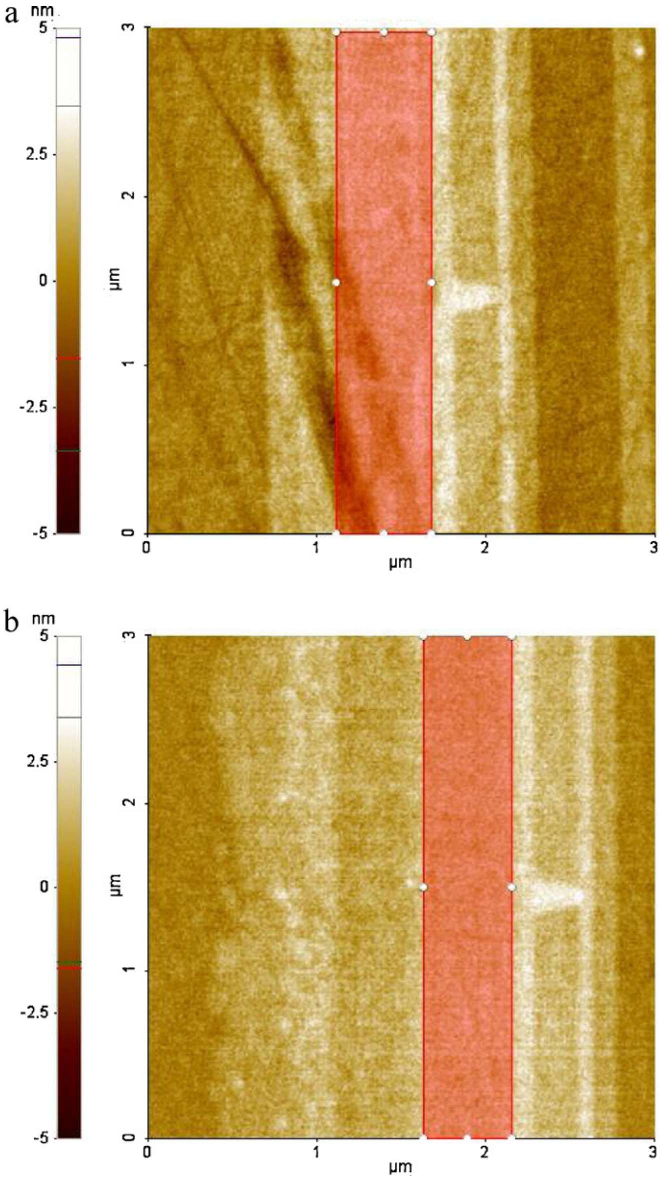

Fig. 9. 3 μm × 3 μm AFM images of pole tip after nanogrinding with as-received (a) and modified polycrystalline NDs (b).

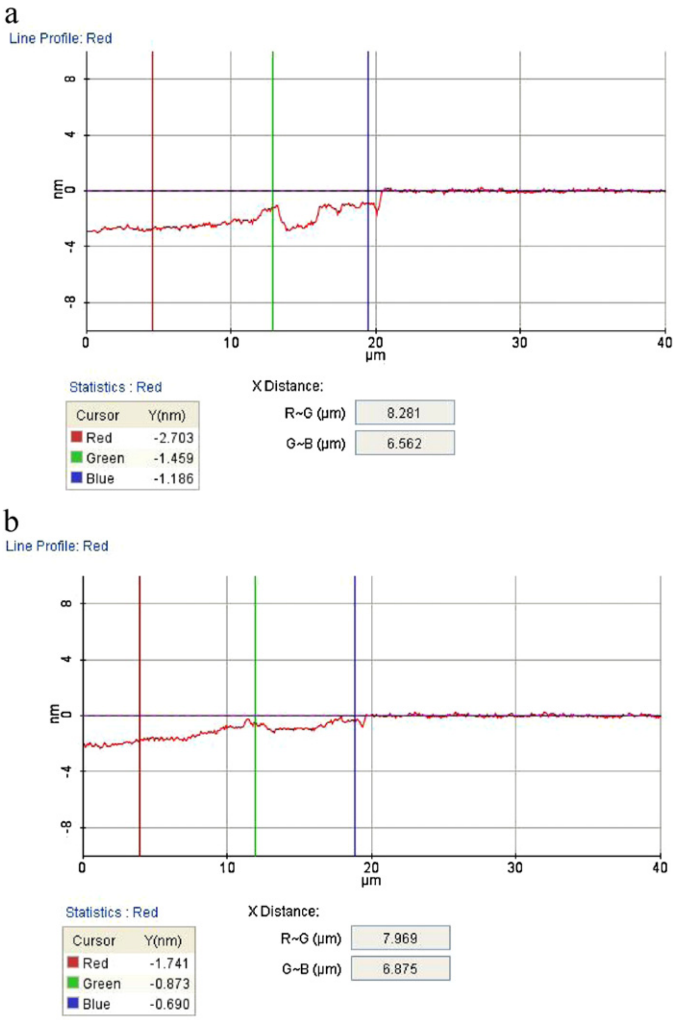

Fig. 10. Pole tip recession of TFH after nanogrinding with as-received polycrystalline NDs (a) and modified one (b).

Another reason for the improvement of nanogrinding surface must be considered. Monocrystalline diamond particles are irregularly shaped and well-faceted. The sharp edges always cut finishing surface with deep microscratch. By comparison, the geometric shape of polycrystalline NDs is sphere-like and the continuous cleavage planes are not present. Then, sub-nanometer smooth pole tip surface are obtained.

Because the pole tip material is softer than the substrate material, it is difficult to avoid the pole tip recession from the substrate [27,30]. Then, pole tip recession is monitored. The line profiles are illustrated in Fig. 10. The lower party on the left of the red vertical line is overcoat, while the higher party is the substrate. The pole tip is ranging from the green line to the blue line. As Fig. 10 shows, the overcoat is lower than the pole tip, while the substrate is a little higher than the pole tip. The height between two positions of the green line and the blue line is defined as *PTR* [27,31]. For TFH after nanogrinding with as-received powders, we can learn from the Fig. 10a that *PTR* is about 0.3 nm, and there are slight nicks on the surface. For TFH after nanogrinding with modified particles, *PTR* is nearly zero. Not only corrosion and damage on the pole tip are avoided, but also black blemishes and nicks are free from the surface.

In light of the move pattern of grains, material can be removed in two different ways: fatigue and micro-cutting [32]. Hard brittle material is apt to be removed by fatigue while ductile material is more easily to be removed by micro-cutting. When the load or size of diamond particles is larger than critical value, the brittle ceramic material will be removed because of indentation fracture [33], which must be avoided. In nanogrinding, since diamond particles are embedded in the tin plate and there is not any free abrasive in the lubricant, the wear condition can be controlled well and the grains only move in two body abrasive way. Then, sub-nanometer smooth and planar TFH surface could be achieved. For a prepared tin plate, Rulin Shen et al. [19] speculated that TFH could be removed uniformly in micro-cutting way. The substrate bears more pressure in nanogrinding than pole tip area for the pole tip is recessed in the former lapping process. More pressure leads to more removal rate. In this way, the *PTR* can be reduced.

4. Conclusion

Well-dispersed and stable suspensions of polycrystalline NDs in clean oil medium can be prepared by modifying the nanoparticles with PMF enhanced H_2 plasma in the gas phase. FTIR date well evidences the removal of the oxygenated groups initially presented on polycrystalline NDs surface. The treatment modifies the surface of the polycrystalline NDs without altering their crystalline sp^3 diamond core. The enhancement of PMF on H_2 plasma modification can be attributed to magnetic field confinement with the electrons emitted from the hot filament. TFH nanogrinding with the suspension validates its dispersion behavior. Sub-nanometer smooth pole tip surface and planar recording surface are achieved.

References

[1] O.V. Turova, E.V. Starodubtseva, M.G. Vinogradov, V.I. Sokolov, N.V. Abramova, A.Y. Vul, A.E. Alexenskiy, Palladium supported on detonation nanodiamond as a highly effective catalyst of the $C=C$ and $C\equiv C$ bond hydrogenation, Catal. Commun. 12 (2011) 577–579.

[2] A. Krueger, Beyond the shine: recent progress in applications of nanodiamond, J. Mater. Chem. 21 (2011) 12571–12578.

[3] Y.V. Butenko, P.R. Coxon, M. Yeganeh, A.C. Brieva, K. Liddell, V.R. Dhanak, L. Šiller, Stability of hydrogenated nanodiamonds under extreme ultraviolet irradiation, Diamond Relat. Mater. 17 (2008) 962–966.

[4] S. Michaelson, A. Stacey, R. Akhvlediani, S. Prawer, A. Hoffman, High resolution electron energy loss spectroscopy surface studies of hydrogenated detonation nano-diamond spray-deposited films, Surf. Sci. 604 (2010) 1326–1330.

[5] X. Liu, T. Yu, Q. Wei, Z. Yu, X. Xu, Enhanced diamond nucleation on copper substrates by employing an electrostatic self-assembly seeding process with modified nanodiamond particles, Colloid Surface A 412 (2012) 82–89.

[6] V. Chakrapani, J.C. Angus, A.B. Anderson, S.D. Wolter, B.R. Stoner, G.U. Sumanasekera, Charge transfer equilibria between diamond and an aqueous oxygen electrochemical redox couple, Science 318 (2007) 1424–1430.

[7] C.E. Nebel, B. Rezek, D. Shin, H. Watanabe, Surface electronic properties of H-terminated diamond in contact with adsorbates and electrolytes, Phys. Status Solidi (A) 203 (2006) 3273–3298.

[8] W. Hongthani, N.A. Fox, D.J. Fermiĭn, Electrochemical properties of two dimensional assemblies of insulating diamond particles, Langmuir 27 (2011) 5112–5118.

[9] M. Yeganeh, P.R. Coxon, A.C. Brieva, V.R. Dhanak, L. Šiller, Y.V. Butenko, Atomic hydrogen treatment of nanodiamond powder studied with photoemission spectroscopy, Phys. Rev. B 75 (2007) 155404.

[10] W.S. Yeap, S. Chen, K.P. Loh, Detonation nanodiamond: an organic platform for the Suzuki coupling of organic molecules, Langmuir 25 (2008) 185–191.

[11] H.A. Girard, J.C. Arnault, S. Perruchas, S. Saada, T. Gacoin, J.P. Boilot, P. Bergonzo, Hydrogenation of nanodiamonds using MPCVD: a new route toward organic functionalization, Diamond Relat. Mater. 19 (2010) 1117–1123.

[12] S. Koizumi, C. Nebel, M. Nesladek, Physics and Applications of CVD Diamond, John Wiley & Sons, 2008, p. 32.

[13] X. You, Z. Yu, L. Shi, L. Wang, Influence of periodic magnetic field on the growth of CVD diamond films at lower temperature, J. Cryst. Growth 311 (2009) 4675–4678.

[14] J.B. Donnet, E. Fousson, T.K. Wang, M. Samirant, C. Baras, M. Pontier Johnson, Dynamic synthesis of diamonds, Diamond Relat. Mater. 9 (2000) 887–892.

[15] J.-B. Donnet, É. Fousson, M. Samirant, T.K. Wang, M. Pontier-Johnson, A. Eckhardt, Shock synthesis of nanodiamonds from carbon precursors: identification of carbynes, C. R. Acad. Sci. Ser. IIC: Chem. 3 (2000) 359–364.

[16] P. Chen, F. Huang, S. Yun, Structural analysis of dynamically synthesized diamonds, Mater. Res. Bull. 39 (2004) 1589–1597.

[17] B.R. Rosczyk, L.M. Nagle, I.C. Benea, Nano clustered diamond-characterisation of properties, Ind. Diamond Rev. 1 (2007) 47–52.

[18] H.H. Gatzen, J. Chris Maetzig, Nanogrinding, Precis. Eng. 21 (1997) 134–139.

[19] R.L. Shen, J. Zhong, Ultra Precision Polishing of GMR Hard-Disk Magnetic Head, IEEE, New York, 2006.

[20] C.D. Chu, E. Perevedentseva, V. Yeh, S.J. Cai, J.S. Tu, C.L. Cheng, Temperature-dependent surface CO stretching frequency investigations of functionalized nanodiamond particles, Diamond Relat. Mater. 18 (2009) 76–81.

[21] D.S. Knight, Characterization of diamond films by Raman spectroscopy, J. Mater. Res. 4 (1989) 385–393.

[22] Q. Wei, M.N.R. Ashfold, Y.A. Mankelevich, Z.M. Yu, P.Z. Liu, L. Ma, Diamond growth on WC-Co substrates by hot filament chemical vapor deposition: effect of filament–substrate separation, Diamond Relat. Mater. 20 (2011) 641–650.

[23] V.V. Korolkov, I.I. Kulakova, B.N. Tarasevich, G.V. Lisichkin, Dual reaction capacity of hydrogenated nanodiamond, Diamond Relat. Mater. 16 (2007) 2129–2132.

[24] Y. Zhu, X. Xu, B. Wang, Z. Feng, Surface modification and dispersion of nanodiamond in clean oil, China Particuol. 2 (2004) 132–134.

[25] A. Krueger, T. Boedeker, Deagglomeration and functionalisation of detonation nanodiamond with long alkyl chains, Diamond Relat. Mater. 17 (2008) 1367–1370.

[26] Y. Liu, Z. Gu, J.L. Margrave, V.N. Khabashesku, Functionalization of nanoscale diamond powder: fluoro-, alkyl-, amino-, and amino acid-nanodiamond derivatives, Chem. Mater. 16 (2004) 3924–3930.

[27] M. Jiang, S. Hao, R. Komanduri, On the advanced lapping process in the precision finishing of thin-film magnetic recording heads for rigid disc drives, Appl. Phys. A: Mater. 77 (2003) 923–932.

[28] J.G. Buijnsters, L. Vazquez, G.W.G. van Dreumel, J.J. ter Meulen, W.J.P. van Enckevort, J.P. Celis, Enhancement of the nucleation of smooth and dense nanocrystalline diamond films by using molybdenum seed layers, J. Appl. Phys. 108 (2010) 103514–103519.

[29] J.T. Drotar, Y.P. Zhao, T.M. Lu, G.C. Wang, Numerical analysis of the noisy Kuramoto–Sivashinsky equation in 2 + 1 dimensions, Phys. Rev. E 59 (1999) 177–185.

[30] E. Abenojar, J. Herber, E. Enriquez, Surface energies of magnetic recording head components, Tribol. Lett. 41 (2011) 587–595.

[31] R.-L. Shen, J. Zhong, Ultrasonic polishing of giant magnetic resistance magnetic recording heads for hard discs, Proc. Inst. Mech. Eng. J: J. Eng. Tribol. 223 (2009) 735–737.

[32] L. Fang, X.L. Kong, J.Y. Su, Q.D. Zhou, Movement patterns of abrasive particles in three-body abrasion, Wear 162-164 (Part B) (1993) 782–789.

[33] B.R. Lawn, M.V. Swain, Microfracture beneath point indentations in brittle solids, J. Mater. Sci. 10 (1975) 113–122.